

# Supermassive black hole formation by the cold accretion shocks in the first galaxies

Kohei Inayoshi<sup>1</sup> <sup>\*</sup> and Kazuyuki Omukai<sup>1</sup> <sup>†</sup>

<sup>1</sup>*Department of Physics, Graduate School of Science, Kyoto University, Kyoto 606-8502, Japan*

## ABSTRACT

We propose a new scenario for supermassive star (SMS;  $\gtrsim 10^5 M_\odot$ ) formation in shocked regions of colliding cold accretion flows near the centers of first galaxies. Recent numerical simulations indicate that assembly of a typical first galaxy with virial temperature  $T_{\text{vir}} \gtrsim 10^4$  K proceeds via cold and dense flows penetrating deep to the center, where the supersonic streams collide each other to develop a hot ( $\sim 10^4$  K) and dense ( $\sim 10^3 \text{ cm}^{-3}$ ) shocked gas. The post-shock layer first cools by efficient Ly $\alpha$  emission and contracts isobarically until  $\simeq 8000$  K. Whether the layer continues the isobaric contraction depends on the density at this moment: if the density is high enough for collisionally exciting H<sub>2</sub> rovibrational levels ( $\gtrsim 10^4 \text{ cm}^{-3}$ ), enhanced H<sub>2</sub> collisional dissociation suppresses the gas to cool further. In this case, the layer fragments into massive ( $\gtrsim 10^5 M_\odot$ ) clouds, which collapse isothermally ( $\sim 8000$  K) by the Ly $\alpha$  cooling without subsequent fragmentation. As an outcome, SMSs are expected to form and evolve eventually to seeds of supermassive black holes (SMBH). By calculating thermal evolution of the post-shock gas, we delimit the range of post-shock conditions for the SMS formation, which can be expressed as:  $T \gtrsim 6000$  K ( $n_{\text{H}}/10^4 \text{ cm}^{-3})^{-1}$  for  $n_{\text{H}} \lesssim 10^4 \text{ cm}^{-3}$  and  $T \gtrsim 5000 - 6000$  K for  $n_{\text{H}} \gtrsim 10^4 \text{ cm}^{-3}$ , depending somewhat on initial ionization degree. We found that metal enrichment does not affect the above condition for metallicity below  $\simeq 10^{-3} Z_\odot$  if metals are in the gas phase, while condensation of several percent of metals into dust decreases this critical value of metallicity by an order of magnitude. Unlike the previously proposed scenario for SMS formation, which postulates extremely strong ultraviolet radiation to quench H<sub>2</sub> cooling, our scenario here naturally explains the SMBH seed formation in the assembly process of the first galaxies, even without such a strong radiation.

**Key words:** stars: formation, Population III — dark ages, reionization, first stars — galaxies: formation, nuclei

## 1 INTRODUCTION

Discovery of high- $z$  quasars has demonstrated the existence of supermassive black holes (SMBH) with  $\sim 10^9 M_\odot$  already at the age of the universe  $\lesssim 1$  Gyr (e.g., Fan 2006; Willott et al. 2007; Mortlock et al. 2011). As an origin of such SMBHs, seed BH formation as a remnant of population III stars ( $M_{\text{seed}} \sim 100 M_\odot$ ) and their subsequent growth by merger and gas accretion have been studied by a number of authors (e.g., Haiman & Loeb 2001; Volonteri, Haardt & Madau 2003; Li et al. 2007). Even with the Eddington accretion rate  $\dot{M}_{\text{Edd}} = L_{\text{Edd}}/\epsilon c^2$ , where  $L_{\text{Edd}}$  is the Eddington luminosity and  $\epsilon \simeq 0.1$  is the radiative efficiency, the growth time  $t_{\text{grow}} = 0.05 \ln(M_{\text{BH}}/M_{\text{seed}})$  Gyr becomes as long as the age of the universe at  $z \simeq 6$  ( $\simeq 0.8$  Gyr): the

seed BHs are thus required to keep growing at the Eddington rate. However, negative feedbacks by the growing BHs prevent such efficient accretion (Milosavljević, Couch & Bromm 2009; Alvarez, Wise & Abel 2009; Jeon et al. 2011).

As a solution to this, alternative possibility of massive seed BH formation by direct collapse of supermassive stars (SMS;  $\gtrsim 10^5 M_\odot$ ) has been considered by some authors. Specifically, SMS formation in massive halos ( $T_{\text{vir}} \gtrsim 10^4$  K) irradiated with strong far ultraviolet (FUV) radiation has often been studied (e.g., Bromm & Loeb 2003; Regan & Haehnelt 2009a, b; Shang, Bryan, & Haiman 2010). Since H<sub>2</sub> molecule, the main coolant in the primordial gas, is photodissociated with strong FUV radiation in the Lyman and Werner bands, clouds under such an environment collapse isothermally at  $\sim 8000$  K by Ly $\alpha$  cooling without fragmentation, if they are massive enough with  $\gtrsim 10^5 M_\odot$ . As an outcome of such collapse, SMSs are expected to form. A massive seed BH as a remnant of SMS collapse reduces the growth

<sup>\*</sup> E-mail: inayoshi@tap.scphys.kyoto-u.ac.jp

<sup>†</sup> E-mail: omukai@tap.scphys.kyoto-u.ac.jp

time to  $10^9 M_\odot$  within 0.46 Gyr and mitigates the growth-time problem by a big margin. This scenario, however, has a serious drawback: for this mechanism of SMS formation to work, extremely strong FUV radiation  $J_{21}^{\text{FUV}} \gtrsim 10^2 - 10^3$  (in a unit of  $10^{-21} \text{ erg s}^{-1} \text{ cm}^{-2} \text{ Hz}^{-1} \text{ sr}^{-1}$ ) is required (Omukai 2001; Bromm & Loeb 2003; Shang, Bryan & Haiman 2010), while the fraction of halos irradiated with such intense FUV fields with  $J_{21}^{\text{FUV}} \gtrsim 10^3$  is estimated to be  $\lesssim 10^{-6}$  at  $z \sim 10$  (Dijkstra et al. 2008), i.e., only extremely rare halos satisfy the condition for SMS formation. Moreover, if high energy components, such as cosmic rays or X-rays, are present along with the FUV radiation, their ionization effect promotes the  $\text{H}_2$  formation and then strongly suppresses the SMS formation (Inayoshi & Omukai 2011). Although the above scenario might be still viable considering the rarity of high- $z$  SMBHs, it is worthwhile to explore another possibility.

In this paper, we propose a new scenario for SMS formation in post-shock gas of cold accretion flows in forming first galaxies. Recent numerical simulations of galaxy formation have revealed that, in halos with virial temperature  $T_{\text{vir}} \gtrsim 10^4 \text{ K}$ , the shock position does not stay at the virial radius and shrinks inside owing to the efficient  $\text{Ly}\alpha$  cooling, and the accreting cold gas penetrates deep to the center through dense filamentary flows (Birnboim & Dekel 2003; Kereš et al. 2005; Dekel & Birnboim 2006; Dekel et al. 2009; Bromm & Yoshida 2011). The supersonic flows collide each other and the resultant shock develops a hot and dense ( $\sim 10^4 \text{ K}$  and  $\sim 10^3 \text{ cm}^{-3}$ ) gas near the center (Wise & Abel 2007; Greif et al. 2008; Wise, Turk & Abel 2008). By studying thermal evolution of the shocked gas, we have found that, if the post-shock density is high enough for the  $\text{H}_2$  rovibrational levels to reach the local thermodynamic equilibrium (LTE), the efficient collisional dissociation suppresses  $\text{H}_2$  cooling, and the gas cannot cool below several thousand K. Massive clouds with  $\gtrsim 10^5 M_\odot$  formed by fragmentation of the post-shock layer subsequently collapse isothermally at  $\sim 8000 \text{ K}$  by the  $\text{Ly}\alpha$  cooling. Without further fragmentation, monolithic collapse of the clouds results in the SMS formation. Note that, unlike the previous SMS formation mechanism, strong FUV radiation is not required in our scenario. Similar analysis has also been carried out by Safranek-Shrader, Bromm & Milosavljević (2010), who studied the fragmentation of the cold-stream shocked layer considering the effects of radiation field and chemical enrichment, but for a single post-shock condition ( $4 \times 10^3 \text{ cm}^{-3}$ ,  $1.1 \times 10^4 \text{ K}$ , and the equilibrium chemical abundances).

The organization of this paper is as follows. In Section 2, we describe the model for calculation of thermal evolution in the shocked gas. In Section 3, we present our results and clarify the conditions for isothermal collapse leading to the SMS formation in terms of post-shock density and temperature. Effects of metal enrichment is also considered here. In Section 4, we analyze thermal processes in the shocked gas and discuss the reason for the bifurcation of thermal evolution in more detail. Finally, we summarize our study and present some discussions in Section 5.

## 2 MODEL

In this section, we describe our model for calculation of thermal evolution in hot and dense shocked regions formed by collision of cold accretion flows in the first galaxies.

### 2.1 Evolution in the post-shock layer

We consider the thermal evolution in the post-shock layer under the assumption that the flow is steady and plane-parallel. Since the post-shock temperature is as high as the virial temperature of first-galaxy forming halos ( $T_{\text{vir}} \gtrsim 10^4 \text{ K}$ ), cooling by the  $\text{Ly}\alpha$  emission is efficient early on. The post-shock flow is compressed almost isobarically as long as the gas cools effectively (e.g., Shapiro & Kang 1987). Within the steady-state approximation, the conservation of mass and momentum leads to the following relationships between the density  $\rho_0$ , pressure  $p_0$ , and flow velocity  $v_0$  just behind the shock with those in the post-shock flow  $\rho$ ,  $p$ , and  $v$ :

$$\rho v = \rho_0 v_0, \quad (1)$$

$$\rho v^2 + p = \rho_0 v_0^2 + p_0. \quad (2)$$

Along this flow, we solve the energy equation

$$\frac{dE}{dt} = \frac{p + E}{\rho} \frac{d\rho}{dt} - \Lambda_{\text{net}}, \quad (3)$$

where  $E$  is the internal energy per unit volume,  $d/dt$  is the Lagrangian time derivative, and  $\Lambda_{\text{net}}$  is the net cooling rate per unit volume. Assuming a strong shock and neglecting the thermal pressure in the pre-shock flow,  $p_0 \simeq 3\rho_0 v_0^2$  is satisfied just behind the shock front. Thus, we approximate the right-hand side of equation (2) by  $4\rho_0 v_0^2$ . The cooling term  $\Lambda_{\text{net}}$  includes the radiative cooling by  $\text{H}$ ,  $\text{H}_2$  and  $\text{HD}$ , and cooling/heating associated with chemical reactions. We solve the chemical reactions of primordial gas among the following 14 species;  $\text{H}$ ,  $\text{H}_2$ ,  $\text{e}^-$ ,  $\text{H}^+$ ,  $\text{H}_2^+$ ,  $\text{H}^-$ ,  $\text{He}$ ,  $\text{He}^+$ ,  $\text{He}^{++}$ ,  $\text{D}$ ,  $\text{HD}$ ,  $\text{D}^+$ ,  $\text{HD}^+$ , and  $\text{D}^-$ . We adopt the same coefficients for the cooling/heating and the chemical reactions as in Inayoshi & Omukai (2011) except for omitting the radiative/cosmic-ray ionization and dissociation in this calculation. In studying effects of metal enrichment, we add the cooling by the fine-structure-line emission of  $\text{C}_{\text{II}}$  and  $\text{O}_{\text{I}}$  to the primordial processes described above. Assuming the fraction of metals depleted to dust grains to be the same as in the Galactic interstellar gas, we set the number fractions of  $\text{C}$  and  $\text{O}$  nuclei in the gas phase with respect to  $\text{H}$  nuclei to  $x_{\text{C,gas}} = 0.927 \times 10^{-4} (Z/Z_\odot)$  and  $x_{\text{O,gas}} = 3.568 \times 10^{-4} (Z/Z_\odot)$  (Pollack et al. 1994). We follow Hollenbach & McKee (1989) in calculating the cooling rates of  $\text{C}_{\text{II}}$  and  $\text{O}_{\text{I}}$ . We curtail the  $\text{C}$  and  $\text{O}$  chemistry by simply assuming that all the  $\text{C}$  and  $\text{O}$  are in the states of  $\text{C}_{\text{II}}$  and  $\text{O}_{\text{I}}$ , respectively, from the following consideration: with lower ionization energy (11.26 eV) than  $\text{H}$  atom,  $\text{C}$  is photoionized by weak background radiation and in the state of  $\text{C}_{\text{II}}$ , while  $\text{O}$  is in ionization equilibrium with  $\text{H}$  and almost neutral for  $\lesssim 8000 \text{ K}$ , where the  $\text{O}_{\text{I}}$  cooling is important. Molecular cooling of metals (e.g.,  $\text{CO}$  and  $\text{H}_2\text{O}$ ) is not included since its cooling is not important in the temperature range relevant for the bifurcation of thermal evolution ( $\gtrsim$  several  $10^3 \text{ K}$ ).

Next, we consider the condition for the gravitational instability during the isobaric compression of the post-shock

layer and thus for its fragmentation. For the isobaric compression, the dynamical time  $t_{\text{dyn}} (\equiv \rho/(d\rho/dt))$ , which characterizes thermal evolution, is approximately equal to the cooling time

$$t_{\text{cool}} = \frac{(3/2)n_{\text{H}}k_{\text{B}}T}{\Lambda_{\text{net}}}, \quad (4)$$

where  $n_{\text{H}}$  is the number density of H nuclei and  $T$  is the temperature. On the other hand, the growth timescale for the gravitational instability is given by the free-fall time (e.g., Larson 1985)

$$t_{\text{ff}} = \sqrt{\frac{32}{3\pi G\rho}}. \quad (5)$$

As long as the cooling is effective enough and so  $t_{\text{cool}} (\simeq t_{\text{dyn}}) \lesssim t_{\text{ff}}$ , the post-shock layer continues to be compressed isobarically. However, once the cooling becomes ineffective and  $t_{\text{cool}}$  exceeds  $t_{\text{ff}}$ , the contraction of the layer halts and a dense layer begins to develop inside the post-shock region. For example, since the growth rate of the baryonic mass in halos of  $\sim 10^8 M_{\odot}$  at  $z \sim 10$  is  $\sim 4 \times 10^{-2} M_{\odot}/\text{yr}$  (Dekel et al. 2009), a gas of  $\gtrsim 10^5 M_{\odot}$  can accumulate in  $\gtrsim 3 \times 10^6$  yrs. If sufficient gas supply is available through the accretion flow, the dense layer eventually satisfies the Jeans criterion, i.e., the sound-crossing time  $t_{\text{cross}}$  becomes longer than the free-fall time ( $t_{\text{cross}} \gtrsim t_{\text{ff}}$ ). The layer then fragments by the gravitational instability to produce Jeans-scale clouds. In this paper, assuming that the continuous gas supply to induce the Jeans instability is available, we estimate the fragmentation mass scale by the condition  $t_{\text{ff}} \sim t_{\text{cool}}$  in accordance with Yamada & Nishi (1998).

## 2.2 Evolution after fragmentation

After fragmentation, the cloud collapses with its self-gravity, and its evolution cannot be modelled as a steady flow anymore. Density evolution in a cloud collapsing by the self-gravity is described by the Penston-Larson self-similar solution (Penston 1969; Larson 1969), which has density profile with a flat core of the Jeans scale and an envelope with the power-law density distribution  $\rho(r) \propto r^{-2}$ . The density in the central core roughly increases in the free-fall timescale. We here calculate the evolution in the central-core part by using a one-zone model, where the density evolution is given by

$$\frac{d\rho}{dt} = \frac{\rho}{t_{\text{ff}}}. \quad (6)$$

Namely, after the condition for fragmentation ( $t_{\text{cool}} \gtrsim t_{\text{ff}}$ ) is satisfied, we switch the density evolution described by equations (1)-(2) to that by equation (6) in our calculation and solve equation (3) for this density evolution.

When the collapse proceeds significantly and the cloud becomes optically thick, the radiative cooling becomes ineffective due to photon trapping. We assume the radius of the core to be half a Jeans length

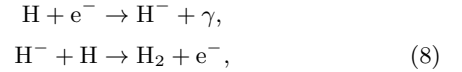
$$R_{\text{c}} = \frac{\lambda_{\text{J}}}{2} = \sqrt{\frac{\pi k_{\text{B}}T}{G\rho\mu m_{\text{H}}}}, \quad (7)$$

where  $\mu$  is the mean molecular weight. Since we consider the core of the collapsing cloud, the column density of  $i$ -th

species is given by  $N_i = x_i n_{\text{H}} R_{\text{c}}$ , where  $x_i$  is its concentration. Using this value, we estimate the optical depth and the reduction rate of radiative cooling as in Inayoshi & Omukai (2011).

## 2.3 Initial conditions

According to numerical simulations of the first galaxy formation (e.g., Greif et al. 2008; Wise et al. 2008), the pre-shock number density and temperature of cold flows and the shock velocity are typically  $10^3 \text{ cm}^{-3}$ , 200 K, and 20 km  $\text{s}^{-1}$ , respectively, which correspond to the post-shock density  $4 \times 10^3 \text{ cm}^{-3}$  and temperature 9000 K. With those fiducial values in mind, we carry out calculations for a wide range of initial number density and temperature:  $10^2 \text{ cm}^{-3} < n_{\text{H},0} < 10^7 \text{ cm}^{-3}$  and  $3000 \text{ K} < T_0 < 10^5 \text{ K}$ . Since  $\text{H}_2$ , the main coolant below 8000 K, forms through the electron-catalyzed reactions



the initial ionization degree  $x_{\text{e},0}$ , along with the initial  $\text{H}_2$  concentration  $x_{\text{H}_2,0}$ , is important quantities for the subsequent thermal evolution. In reference to the results of Kang & Shapiro (1992), who studied the chemical abundances in the pre-shock gas considering photo-ionization and dissociation by UV radiation emitted from the shock, we regard  $x_{\text{e},0} \sim 10^{-2}$  and  $x_{\text{H}_2,0} \sim 10^{-6}$  as typical ionization degree and molecular fraction, respectively. However, since cold accretion flows are far denser ( $\sim 10^3 \text{ cm}^{-3}$ ) than the range Kang & Shapiro (1992) assumed ( $\lesssim 10^{-2} \text{ cm}^{-3}$ ), the electron recombination as well as the shielding of the UV photo-ionization/dissociation probably lower the pre-shock ionization degree  $x_{\text{e},0}$  and elevate molecular fraction  $x_{\text{H}_2}$  from those values. Taking this uncertainty into account, we study the cases with a wide range of initial ionization degree and  $\text{H}_2$  fraction:  $10^{-5} \leq x_{\text{e},0} \leq 10^{-1}$  and  $10^{-6} \leq x_{\text{H}_2,0} \leq 10^{-3}$ .

## 3 RESULTS

In this section, we present our results for thermal evolution after the gas experiences the cold accretion shock. We first consider the cases of primordial gas and then discuss effects of small metal enrichment.

### 3.1 Primordial-gas case

In Fig. 1, we show the temperature evolution of primordial gas for four post-shock conditions, indicated by two each open and filled circles. We here set the initial ionization degree and molecular fraction to  $x_{\text{e},0} = 10^{-2}$  and  $x_{\text{H}_2,0} = 10^{-6}$ , respectively. First, we see the cases from the open-circle initial conditions in Fig. 1, whose temperature evolution is shown by the dashed lines. In the lower initial-density case ( $n_{\text{H},0}, T_0 = (5 \times 10^2 \text{ cm}^{-3}, 3.6 \times 10^4 \text{ K})$ ) among them, the post-shock gas cools by the  $\text{Ly}\alpha$  emission and is compressed isobarically. Although the  $\text{Ly}\alpha$  cooling becomes inefficient below 8000 K, enough  $\text{H}_2$  for cooling has already been formed by this time, which enables further temperature decrease. HD is formed abundantly for  $\lesssim 150 \text{ K}$ , whose

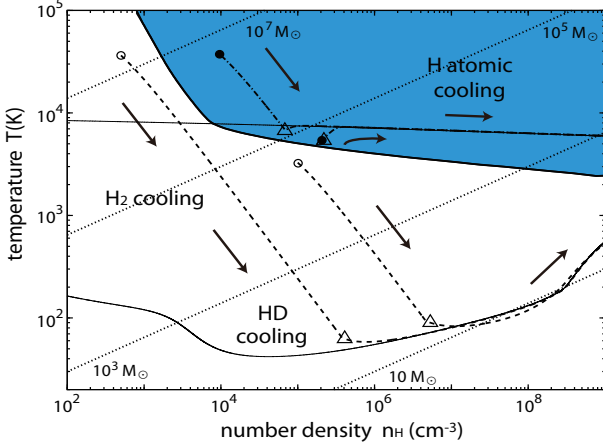


**Figure 1.** The temperature evolution of primordial gas after heated by the cold accretion shock for the initial ionization degree  $x_{e,0} = 10^{-2}$  and  $H_2$  fraction  $x_{H_2,0} = 10^{-6}$ . The evolutionary tracks are shown with dashed and dash-dotted lines for four combinations of initial temperature and density, indicated by two each open and filled circles. From low-density or low-temperature initial conditions (dashed lines starting from the open circles), the temperature decreases below  $\sim 100$  K owing to the  $H_2$  and HD cooling. On the other hand, from dense and hot initial conditions (dash-dotted lines from the filled circles), the clouds do not cool below  $\sim 8000$  K and subsequently collapse almost isothermally by the H atomic cooling. The triangle symbol on each track indicates the epoch when the post-shock layer fragments by the gravitational instability. The thick solid line, the domain above which is hatched, divides the initial conditions leading to these two different ways of thermal evolution. The two thin solid lines show the temperature evolution by the H atomic cooling (upper) and the  $H_2$  and HD cooling (lower), respectively. These two evolutionary tracks are calculated by the density evolution of equation (6) from the initial conditions  $n_{H,0} = 10 \text{ cm}^{-3}$ ,  $T_0 = 10^4 \text{ K}$ , and  $x_{e,0} = 2 \times 10^{-4}$  (upper) and  $10^{-1}$  (lower), respectively. For the upper track, the  $H_2$  cooling rate is set to zero. The diagonal dotted lines (lower-left to upper-right) indicate the constant Jeans masses, whose values are denoted by numbers in the Figure.

cooling eventually lowers the temperature to  $\sim 50$  K. At this point, without efficient coolant anymore,  $t_{\text{cool}}$  becomes longer than  $t_{\text{ff}}$ . Clouds with Jeans mass of several  $10 M_\odot$  are produced by the gravitational instability. Also, in the case of lower initial temperature ( $10^5 \text{ cm}^{-3}$ ,  $3.3 \times 10^3 \text{ K}$ ), abundant  $H_2$  is formed immediately. The cooling by  $H_2$  and then by HD allows the temperature to plummet isobarically until  $\sim 100$  K, where the fragmentation mass scale of a few  $10 M_\odot$  is imprinted. In both the cases, temperature evolution after fragmentation converges to the well-known track for clouds collapsing by the self-gravity and cooling by  $H_2$  and HD (lower thin solid line; Uehara & Inutsuka 2000; Nagakura & Omukai 2005).

Next, we see the two cases starting from the filled-circle initial conditions in Fig. 1, whose evolutionary tracks are indicated by the dash-dotted lines. In the higher initial temperature case ( $10^4 \text{ cm}^{-3}$ ,  $3.6 \times 10^4 \text{ K}$ ), the gas cools isobarically until  $8000$  K as in the open-circle cases. At  $\sim 8000$  K, however, the density exceeds  $\sim 10^4 \text{ cm}^{-3}$ , the critical density for  $H_2$  to reach LTE. For higher density,  $H_2$  is rapidly dissociated collisionally from the excited rovibrational levels, and thus sufficient  $H_2$  for cooling is never formed. Con-

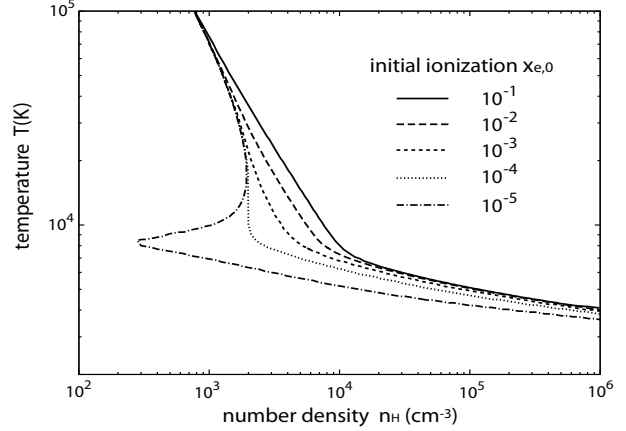


**Figure 2.** The effect of initial ionization degree on the range of post-shock initial conditions leading to isothermal collapse by H atomic cooling and thus SMS formation. The lines present their boundaries for the cases with different initial ionization degrees of  $x_{e,0} = 10^{-1}$  (solid),  $10^{-2}$  (long-dashed),  $10^{-3}$  (short-dashed),  $10^{-4}$  (dotted), and  $10^{-5}$  (dash-dotted), respectively. The molecular fraction  $x_{H_2,0} = 10^{-6}$  for all cases.

sequently, the gas cannot cool below  $\sim 8000$  K, and massive clouds with  $\gtrsim 10^5 M_\odot$  are formed by fragmentation. Also, in the case of initial temperature somewhat lower than  $8000$  K ( $2 \times 10^5 \text{ cm}^{-3}$ ,  $5 \times 10^3 \text{ K}$ ),  $H_2$  cooling is suppressed by the collisional dissociation and fragmentation occurs immediately producing massive clouds with  $\gtrsim 10^5 M_\odot$ , whose temperature increases to  $8000$  K by the compressional heating in the course of gravitational collapse. In both cases, the massive clouds thereafter collapse almost isothermally by the Ly $\alpha$  cooling until very high density ( $\sim 10^{16} \text{ cm}^{-3}$ ), where the cloud becomes optically thick to the  $H^-$  bound-free absorption (Omukai 2001). Such isothermally contracting clouds do not fragment in the later phase and thus collapse monolithically to SMSs, which eventually evolve to seeds of SMBHs (Bromm & Loeb 2003; Shang, Bryan & Haiman 2010).

As seen above, the behaviors of thermal evolution can be classified into two types. The thick solid line in Fig. 1 corresponds to the boundary of initial conditions, from the above or below which subsequent thermal evolution bifurcates. Namely, the post-shock conditions above the boundary (the hatched region) lead to the isothermal evolution at  $\sim 8000$  K, while those below it result in the isobaric temperature decrease until  $\lesssim 100$  K. The boundary on the low-density side ( $n_{H,0} \lesssim 10^4 \text{ cm}^{-3}$ ) can be fitted as

$$T_0 \gtrsim 8 \times 10^3 \left( \frac{n_{H,0}}{7 \times 10^3 \text{ cm}^{-3}} \right)^{-1} \text{ K}. \quad (9)$$

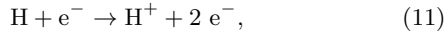
This means that, after isobaric cooling to  $8000$  K, if the density exceeds the  $H_2$  critical value for LTE ( $\sim 10^4 \text{ cm}^{-3}$ ), the gas cannot continue further isobaric compression and starts isothermal collapse. For higher densities  $n_{H,0} \gtrsim 10^4 \text{ cm}^{-3}$ , the boundary is given by

$$T_0 \gtrsim 5 \times 10^3 \left( \frac{n_{H,0}}{10^5 \text{ cm}^{-3}} \right)^{-0.1} \text{ K}. \quad (10)$$

In Section 4, we discuss physical processes determining the location of the boundary in more detail.

We mention the effect of initial chemical composition on thermal evolution. In Fig. 2, we show the boundaries

for the SMS-forming conditions for different initial ionization degrees ( $10^{-5} \leq x_{e,0} \leq 10^{-1}$ ). The positions of the boundaries are almost independent of  $x_{e,0}$  for  $\gtrsim 10^4 \text{ cm}^{-3}$ , while the portions at  $\lesssim 10^4 \text{ cm}^{-3}$  move to lower density with decreasing  $x_{e,0}$ . In particular, for  $x_{e,0} = 10^{-5}$ , this results in the spiky domain around 8000 K extending as low as  $\sim 3 \times 10^2 \text{ cm}^{-3}$ . With the higher initial ionization degree, the more  $\text{H}_2$  is formed by the electron-catalyzed reactions (8), which results in the wider range of post-shock conditions for  $\text{H}_2$  cooling, i.e., the smaller range for SMS formation. The boundary for  $x_{e,0} \leq 10^{-2}$  asymptotically approaches that for higher  $x_{e,0}$  at  $\gtrsim 3 \times 10^4 \text{ K}$  since the ionization degree jumps up immediately to  $\sim 10^{-1}$ , even with smaller initial value, by effective collisional ionization



in this temperature range. We also studied the cases with different molecular fraction  $x_{\text{H}_2,0} = 10^{-6}, 10^{-4}$  and  $10^{-3}$ , and found that the boundaries for SMS formation is almost independent of  $x_{\text{H}_2,0}$ . This is because, even with high initial value,  $\text{H}_2$  is rapidly dissociated collisionally for  $\lesssim 10^4 \text{ cm}^{-3}$ , and its fraction reaches the equilibrium one, which is independent of initial value.

### 3.2 Metallicity effect

Next, we consider the cases with slight metal enrichment. In Fig. 3, we present the boundaries for SMS-forming initial conditions for various metallicities with  $0 \leq Z \leq 2 \times 10^{-3} Z_\odot$ . With some metals, cooling by the fine-structure line emission of  $\text{C II}$  and  $\text{O I}$  can exceed that by  $\text{H}_2$  and plays an important role in thermal evolution. With metallicity as low as  $Z \lesssim 5 \times 10^{-4} Z_\odot$ , the metal cooling does not affect thermal evolution around 8000 K and the boundary does not move from the primordial case. As seen in Section 3.1, from initial conditions hotter and denser than the boundary (i.e., the hatched region of Fig. 1), enough  $\text{H}_2$  for cooling is not formed and only massive clouds are produced, which collapse isothermally thereafter. With increasing metallicity, the metal-line cooling becomes able to make the gas to cool below  $\sim 5000 \text{ K}$  isobarically even without  $\text{H}_2$ . Once the temperature decreases and the collisional dissociation becomes ineffective, abundant  $\text{H}_2$  eventually forms and the gas cools to  $\lesssim 100 \text{ K}$  by its cooling. By this additional cooling, the boundary of the SMS-forming initial conditions moves to higher density. With metallicity as high as  $Z \sim 10^{-3} Z_\odot$ , the cooling rate by  $\text{C II}$  and  $\text{O I}$  becomes comparable to the compressional heating at  $\sim 8000 \text{ K}$  and  $\sim 10^4 \text{ cm}^{-3}$ . Therefore, even without help of  $\text{H}_2$  cooling, the metal cooling alone is able to lower the temperature to the range where the  $\text{H}_2$  collisional dissociation is ineffective, and thus the boundary shifts to higher density.

In summary, with metallicity higher than the critical value  $Z_{\text{cr}} \sim 10^{-3} Z_\odot$ , the boundary density becomes far higher than the typical post-shock value by the cold accretion shock  $\sim 10^3 \text{ cm}^{-3}$  and such an initial condition would be very difficult to be realized. Thus the possibility of SMS formation is strongly reduced for higher metallicity. On the other hand, as long as  $Z < Z_{\text{cr}}$ , the range of initial conditions for SMS formation remains the same as in the primordial case.

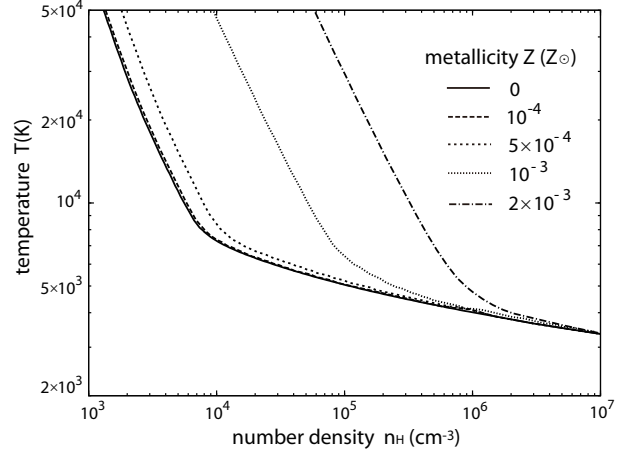


**Figure 3.** The effect of metallicity on the range of post-shock initial conditions leading to SMS formation. The lines present their boundaries for the cases of metallicity  $Z = 0$  (solid),  $10^{-4}$  (long-dashed),  $5 \times 10^{-4}$  (short-dashed),  $10^{-3}$  (dotted),  $2 \times 10^{-3} Z_\odot$  (dot-dashed), respectively. With metallicity higher than  $Z_{\text{cr}} = 10^{-3} Z_\odot$ , the boundary remarkably shifts toward higher density. The initial ionization degree and molecular fraction are  $x_{e,0} = 10^{-2}$  and  $x_{\text{H}_2,0} = 10^{-6}$ , respectively.

## 4 MECHANISM FOR THE BIFURCATION OF THERMAL EVOLUTION

In this Section, we explain what processes are responsible for the bifurcation of thermal evolution in the region where the cold accretion shock is thermalized, and give a physical interpretation for the location of the bifurcation boundary for the post-shock conditions in Figs. 1 and 2.

Efficient  $\text{Ly}\alpha$  cooling drives temperature in a hot gas rapidly to  $\simeq 8000 \text{ K}$ , where its cooling rate is sharply cut off as the atomic hydrogen is not excited for lower temperature. In Fig. 4, we show the cut-off temperature (dotted line), below which  $\text{H}_2$  takes over the role of the dominant coolant. Thus, for the post-shock gas to continue the isobaric cooling below 8000 K, the  $\text{H}_2$  cooling must become effective and keep the cooling time  $t_{\text{cool}}$  shorter than the free-fall time  $t_{\text{ff}}$ . The cooling time by the  $\text{H}_2$  cooling is given by

$$t_{\text{cool}} = \frac{(3/2)k_{\text{B}}T}{\mathcal{L}_{\text{H}_2 x_{\text{H}_2}}}, \quad (12)$$

where  $\mathcal{L}_{\text{H}_2} = \Lambda_{\text{H}_2}/(n_{\text{H}}x_{\text{H}_2})$  is the cooling rate per an  $\text{H}_2$  molecule ( $\text{erg s}^{-1}$ ) and has the density dependence  $\mathcal{L}_{\text{H}_2} \propto (1 + n_{\text{H},\text{cr}}/n_{\text{H}})^{-1}$  ( $n_{\text{H},\text{cr}} \simeq 10^4 \text{ cm}^{-3}$  is the  $\text{H}_2$  critical density for LTE). In conditions under consideration (below the dotted line of Fig. 4), the  $\text{H}_2$  fraction  $x_{\text{H}_2}$  is set by the equilibrium between the electron-catalyzed formation reaction and collisional dissociation reaction<sup>1</sup>, and so

$$x_{\text{H}_2} = \frac{k_{\text{form}}}{k_{\text{cd}}} x_{\text{e}}, \quad (13)$$

<sup>1</sup> Only with high  $x_{\text{e}} \sim 10^{-1}$ , the charge exchange reaction ( $\text{H}_2 + \text{H}^+ \rightarrow \text{H}_2^+ + \text{H}$ ) becomes the main dissociation reaction of  $\text{H}_2$  at  $\lesssim 10^3 \text{ cm}^{-3}$ . However, since the bifurcation boundary for  $x_{e,0} = 10^{-1}$  locates at higher density ( $\gtrsim 10^4 \text{ cm}^{-3}$ ), the charge exchange reaction does not have any influences on the location of the boundary. Thus, we adopt equation (13) even for  $x_{\text{e}} \sim 10^{-1}$ .

where  $k_{\text{form}}$  ( $\text{H} + \text{e}^- \rightarrow \text{H}^- + \gamma$ ) and  $k_{\text{cd}}$  ( $\text{H}_2 + \text{H} \rightarrow 3\text{H}$ ) are reaction rate coefficients for the indicated reactions, respectively. Note that  $k_{\text{cd}}$  depends on the fraction of  $\text{H}_2$  in excited states and thus on the density. The rate coefficient  $k_{\text{cd}}$  significantly increases with density near the  $\text{H}_2$  critical density  $n_{\text{H},\text{cr}}$ , which results in the rapid decrease of  $x_{\text{H}_2}$  by the effective collisional dissociation at  $\gtrsim 10^3 \text{ cm}^{-3}$ .

Furthermore, since  $x_{\text{H}_2}$  is proportional to  $x_{\text{e}}$ , the recombination also can be a key reaction to determine  $t_{\text{cool}}$  ( $\propto x_{\text{e}}^{-1}$ ) at  $\lesssim 8000 \text{ K}$ . Since the recombination time  $t_{\text{rec}}$  ( $= 1/\alpha_{\text{rec}} n_{\text{H}} x_{\text{e}}$ ;  $\alpha_{\text{rec}}$  is the recombination rate coefficient) has the same dependence on  $x_{\text{e}}$  as  $t_{\text{cool}}$ , the ratio of these two timescales becomes independent of  $x_{\text{e}}$  and is approximately given by

$$\frac{t_{\text{cool}}}{t_{\text{rec}}} = \frac{(3/2)n_{\text{H}}k_{\text{B}}T}{\mathcal{L}_{\text{H}_2}} \frac{k_{\text{cd}}\alpha_{\text{rec}}}{k_{\text{form}}} \simeq 0.9 \left( \frac{T}{5000 \text{ K}} \right)^{9.0} \left( \frac{n_{\text{H}}}{10^4 \text{ cm}^{-3}} \right). \quad (14)$$

The last expression above is valid for the density and temperature around  $t_{\text{cool}} \simeq t_{\text{rec}}$  and  $\gtrsim 10^4 \text{ cm}^{-3}$ , and the large temperature dependence of equation (14) is due to that of  $k_{\text{cd}}$ . In Fig. 4, we show the range of the parameters satisfying  $t_{\text{cool}} > t_{\text{rec}}$  (the hatched region), where the recombination effectively works during the isobaric contraction. Note that the hatched region appears only at  $\gtrsim 10^3 \text{ cm}^{-3}$ , where  $k_{\text{cd}}$  is enhanced significantly. On the other hand, the ionization degree is frozen during the isobaric compression at the density lower than the hatched region as  $t_{\text{cool}} < t_{\text{rec}}$ . Under constant  $x_{\text{e}}$ , the cooling time becomes shorter and shorter with decreasing temperature as  $t_{\text{cool}} \propto T^{9.7}$  (at  $\simeq 5000 \text{ K}$ ) because the collisional dissociation is strongly suppressed for lower temperature. Thus the efficient  $\text{H}_2$  cooling and resultant isobaric evolution continue until  $\sim 100 \text{ K}$ .

We first consider the cases with  $x_{\text{e},0} \gtrsim 10^{-4}$  and defer the discussion for the lower ionization cases later. As an example, in Fig. 4 we present the evolutionary tracks of the shocked gas with  $x_{\text{e},0} = 10^{-2}$  for different initial temperatures (solid lines) and the bifurcation boundary of the SMS-forming initial condition (right dashed line). While the gas passes through the hatched region where  $t_{\text{rec}} > t_{\text{cool}}$ , the ionization degree and thus  $\text{H}_2$  fraction fall rapidly. If such a gas runs out of  $\text{H}_2$  before reaching the region where  $t_{\text{cool}} < t_{\text{rec}}$ , the condition for fragmentation  $t_{\text{cool}} \gtrsim t_{\text{ff}}$  is immediately satisfied and the clouds formed in this way collapse isothermally thereafter (the solid lines starting from the filled circles in Fig. 4). However, there is a small margin of the initial parameter range above the line  $t_{\text{cool}} = t_{\text{rec}}$  from which the gas manages to maintain a small fraction of  $\text{H}_2$  and can reach the region where  $t_{\text{cool}} < t_{\text{rec}}$ . In this case, the post-shock layer can continue the isobaric contraction until  $\sim 100 \text{ K}$  (the solid line starting from the open circle in Fig. 4). In summary, if the fragmentation condition  $t_{\text{cool}} \gtrsim t_{\text{ff}}$  is met in the range where  $t_{\text{rec}} < t_{\text{cool}}$ , the post-shock layer cannot cool further and clouds formed at this moment begin the isothermal collapse. The set of initial conditions from which the evolutionary tracks meet the condition  $t_{\text{ff}} = t_{\text{cool}}$  just on the line  $t_{\text{rec}} = t_{\text{cool}}$  corresponds to the boundary for the SMS formation in Fig. 1 in the high density regime (i.e., equation 10). Note that the boundary given by equation (10) reflects the density-temperature relation of  $t_{\text{rec}} = t_{\text{cool}}$ , which is mainly determined by the temperature dependence

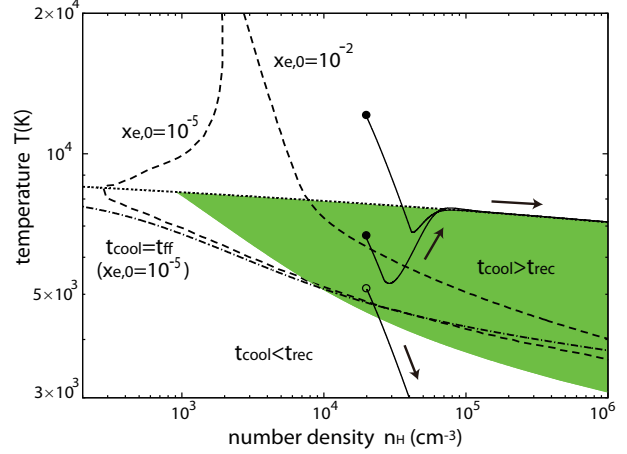


**Figure 4.** The diagram showing relevant processes in setting the bifurcation of the thermal evolution of the shocked gas. The solid lines show the evolutionary tracks of the shocked gas with  $x_{\text{e},0} = 10^{-2}$ , whose post-shock conditions are  $n_{\text{H},0} = 2 \times 10^4 \text{ cm}^{-3}$  and  $T_0 = 1.2 \times 10^4$ ,  $6.6 \times 10^3$ , and  $5.1 \times 10^3 \text{ K}$ , respectively. Two dashed lines present the bifurcation boundaries of the SMS-forming initial conditions for  $x_{\text{e},0} = 10^{-2}$  and  $10^{-5}$ , respectively. The dotted line is the same as the upper thin line in Fig. 1, which corresponds to the cut-off temperature below which the  $\text{H}_2$  line-emission becomes the main cooling process instead of the  $\text{Ly}\alpha$  emission. In the hatched region, the ionization degree rapidly falls by effective recombination within the cooling time of  $\text{H}_2$  ( $t_{\text{cool}} > t_{\text{rec}}$ ). The dot-dashed line presents the condition of  $t_{\text{ff}} = t_{\text{cool}}$  for  $x_{\text{e}} = 10^{-5}$ . Here, the cooling time  $t_{\text{cool}}$  is evaluated by using equation (13).

of  $k_{\text{cd}}$ . Due to the strong dependence of  $k_{\text{cd}}$  on temperature, the  $\text{H}_2$  is collisionally dissociated very efficiently for the temperature higher than given by equation (10). On the other hand, if the density is lower than the  $\text{H}_2$  critical density  $n_{\text{H},\text{cr}}$  ( $\sim 10^4 \text{ cm}^{-3}$ ) after cooling isobarically to  $8000 \text{ K}$ , the gas continues further isobaric contraction to several  $100 \text{ K}$  by the ineffective collisional dissociation of  $\text{H}_2$ . This explains the fact that the low-density side of the boundary of SMS-forming parameters in Fig. 1 (i.e., equation 9) corresponds to the isobaric contraction track whose density at  $\simeq 8000 \text{ K}$  is  $\sim 10^4 \text{ cm}^{-3}$ .

Next, we consider the low ionization cases with  $x_{\text{e},0} \lesssim 10^{-4}$ . As seen in Fig. 4, the portion of the bifurcation boundary (left solid line) for  $x_{\text{e},0} = 10^{-5}$  locates in the region  $t_{\text{rec}} > t_{\text{cool}}$ , where  $x_{\text{e}}$  is frozen during the isobaric compression. Therefore, if the cooling condition  $t_{\text{cool}} < t_{\text{ff}}$  is initially satisfied in the post-shock layer, the gas continues to cool isobarically until  $\lesssim 100 \text{ K}$ , where it produces  $\sim 10 M_{\odot}$  fragments. Thus, the boundary of the SMS-forming condition is simply given by the requirement  $t_{\text{ff}} \lesssim t_{\text{cool}}$  for their initial values without the need for considering the recombination effect. The dot-dashed line in Fig. 4 presents the condition  $t_{\text{ff}} = t_{\text{cool}}$  for  $x_{\text{e}} = 10^{-5}$  and in fact coincides with the boundary on the low-temperature side ( $\lesssim 8000 \text{ K}$ ).

## 5 CONCLUSION AND DISCUSSION

In this paper, we have proposed a new scenario for super-massive star (SMS) formation in central hot and dense re-



gions of the halos formed by the cold accretion shocks in the first galaxy formation. Since the gas cools effectively by Ly $\alpha$  emission in halos with virial temperature  $T_{\text{vir}} \gtrsim 10^4$  K, location of the accretion shock does not stay at the virial radius and shrinks inward. The gas instead flows supersonically along cold and dense filaments to the central region of the first galaxy, where the flows collide each other to produce a hot ( $\gtrsim 10^4$  K) and dense ( $\gtrsim 10^3 \text{ cm}^{-3}$ ) material by a shock (Birnboim & Dekel 2003; Kereš et al. 2005; Dekel & Birnboim 2006; Wise & Abel 2007; Greif et al. 2008; Wise et al. 2008; Dekel et al. 2009; Bromm & Yoshida 2011). We have calculated thermal evolution in such a hot and dense region formed by the cold accretion shock. For  $\gtrsim 8000$  K, the efficient Ly $\alpha$  cooling allows the post-shock gas to cool and to contract isobarically at the value of ram pressure from the shock front. To continue the isobaric cooling also below 8000 K, abundant H $_2$  needs to be formed and its cooling must be effective. If the density at  $\simeq 8000$  K is high enough ( $\gtrsim 10^4 \text{ cm}^{-3}$ ) to make the H $_2$  rovibrational levels to reach the local thermodynamic equilibrium, the H $_2$  is dissociated effectively by the collisional reaction from excited levels, which suppresses the cooling to lower temperature by H $_2$ . At this epoch, gravitational instability of the post-shock layer produces massive fragments with  $\gtrsim 10^5 M_\odot$ , which subsequently collapse isothermally at  $\sim 8000$  K by the Ly $\alpha$  cooling. We have studied thermal evolution of the post-shock gas for a wide range of initial conditions ( $10^2 \text{ cm}^{-3} < n_{\text{H},0} < 10^7 \text{ cm}^{-3}$  and  $3000 \text{ K} < T_0 < 10^5 \text{ K}$ ) and have pinned down the conditions leading to the isothermal collapse (the hatched region in Fig. 1):  $T_0 \gtrsim 6000 (n_{\text{H},0}/10^4 \text{ cm}^{-3})^{-1} \text{ K}$  for  $n_{\text{H},0} \lesssim 10^4 \text{ cm}^{-3}$  and  $T_0 \gtrsim 5000 - 6000 \text{ K}$  for  $n_{\text{H},0} \gtrsim 10^4 \text{ cm}^{-3}$ , for the pre-shock ionization degree at  $x_{\text{e},0} = 10^{-2}$ . Since H $_2$  is formed by the electron-catalyzed reactions (eq. 8), the above condition depends somewhat on the initial ionization degree (see Fig. 2): for smaller  $x_{\text{e},0}$ , the domain of initial conditions leading to the isothermal collapse extends towards lower density. Those massive clouds continue isothermal collapse until very high density  $\sim 10^{16} \text{ cm}^{-3}$ , where they become optically thick to the H $^-$  bound-free absorption (Omukai 2001). The clouds are supposed to collapse directly to SMSs without further fragmentation (e.g., Bromm & Loeb 2003; Regan & Haehnelt 2009a, b; Shang, Bryan, & Haiman 2010). Eventually, the SMSs collapse by the post-Newtonian instability, swallowing most of their material, to become seeds of SMBHs (Shibata & Shapiro 2002).

The first galaxies may be enriched with metals to some extent as well as dusts dispersed by supernova (SN) explosions of previous generations of stars. With high enough metallicity, the gas can cool to low temperature ( $\sim 100$  K) by metal-line cooling alone even without H $_2$ . In this case, the SMS formation would be strongly suppressed. We have then repeated the same analysis by considering as well as the metal cooling by C II and O I. We have found that as long as the metallicity is lower than  $Z_{\text{cr}} \simeq 10^{-3} Z_\odot$ , the metal-line cooling does not change the condition for SMS formation from that in the primordial case (see Fig. 3). According to some cosmological simulations of the assembly of first galaxies (Greif et al. 2010; Wise et al. 2012), the dense gas at the center of galaxies is uniformly enriched to  $\sim 10^{-3} Z_\odot$  by a pair instability SN of massive population III stars with  $140 M_\odot \lesssim M \lesssim 260 M_\odot$ . On the other hand, typical

population III stars are recently considered to be less massive  $\sim 40 M_\odot$  (Hosokawa et al. 2011; Stacy, Greif & Bromm 2011) and end their lives as ordinary core collapse SNe. In this case, the resultant metallicity reduces by a factor of  $\sim 10$  (Heger & Woosley 2002; Nomoto et al. 2006) and thus becomes lower than the critical metallicity for SMS formation we estimated.

We here stress that our scenario naturally explains the formation of seed BHs in the conditions of first-galaxy formation without invoking extremely strong UV radiation as envisaged in the previous scenario. The necessary condition for SMS formation in halos with  $T_{\text{vir}} \gtrsim 10^4$  K is the isothermal collapse by the atomic cooling as a result of suppression of the H $_2$  cooling in the entire density range. So far, as a mechanism to suppress H $_2$  cooling, photodissociation by FUV radiation has been considered. In this scenario, however, extremely strong FUV intensity  $J_{21}^{\text{LW}} \gtrsim 10^2 - 10^3$  (in unit of  $10^{-21} \text{ erg s}^{-1} \text{ cm}^{-2} \text{ Hz}^{-1} \text{ sr}^{-1}$ ) is required to quench the H $_2$  cooling (Omukai 2001; Bromm & Loeb 2003; Shang, Bryan & Haiman 2010), and halos irradiated by such intense radiation are extremely rare ( $\lesssim 10^{-6}$  at  $z \sim 10$ ; Dijkstra et al. 2008). Moreover, if external ionization by cosmic rays or X-rays, which promotes the H $_2$  formation, is present as well, the FUV intensity needed for SMBH formation is elevated. There would be little possibility ( $\ll 10^{-6}$ ) for such an intense FUV field to be realized in any haloes and thus the SMS formation could strongly suppressed (Inayoshi & Omukai 2011). On the other hand, in our scenario, collisional dissociation, rather than photodissociation, suppresses the H $_2$  cooling. Thus, even without FUV radiation, which has been considered to be indispensable previously, the isothermal collapse and thus SMS formation can be realized as long as the right condition is met for the cold accretion shock. Note, however, this mechanism for SMS formation cannot operate in all first galaxies since SMBHs are rare objects. If we use the number density of halos with mass  $\sim 10^8 M_\odot$  at  $z \sim 10$ ,  $\sim 10 \text{ Mpc}^{-3}$  (comoving) and assume each of them had a SMS of  $\sim 10^5 M_\odot$ , the predicted mass density of SMBHs  $\sim 10^6 M_\odot \text{ Mpc}^{-3}$  (comoving) will exceed the total present-day BH mass density  $\sim 3 \times 10^5 M_\odot \text{ Mpc}^{-3}$  estimated by Yu & Tremaine (2002). Therefore, our conditions for SMS formation would be satisfied only in a small fraction of first galaxies or some other processes, e.g., turbulent fragmentation, lack of accreting material etc., suppress this mechanism to work for avoiding overproduction of BHs.

We here briefly discuss the effect of dust cooling, which has not been considered in this paper. If the depletion factor of metals to dust grains is as high as the present-day Galactic value  $f_{\text{dep}} \simeq 0.5$ , the thermal evolution deviates from the isothermal one at  $\gtrsim 10^{10} \text{ cm}^{-3}$  due to the dust cooling, if metallicity is higher than  $Z_{\text{cr,dust}} \simeq 10^{-5} Z_\odot$  (Omukai, Schneider & Haiman 2008). Although this critical metallicity  $Z_{\text{cr,dust}}$  is smaller than the critical value due to metal-line cooling  $Z_{\text{cr}} \simeq 10^{-3} Z_\odot$  by two orders of magnitude, the depletion factor in the first-galaxy forming environment is highly uncertain. According to theoretical models of dust formation and destruction in the first SNe, typically only a few % of dust formed at the explosion survives, after being swept by the reverse shock, depending on the ambient density (Nozawa, Kozasa & Habe 2006; Bianchi & Schneider 2007). For example, with  $f_{\text{dep}} \simeq 0.05$ , the critical metallicity becomes  $Z_{\text{cr,dust}} \simeq 10^{-4} Z_\odot$ , which makes the constraint on

metal pollution less severe. In any case, to predict whether the isothermal collapse continues in spite of metal enrichment, we need more accurate knowledge of the depletion factor  $f_{\text{dep}}$ .

In this paper, we consider the hot and dense central regions owing to shocks by the cold accretion flows in the forming first galaxies. Likewise, a galaxy merging event drives inflows, creating a similar environment around the galaxy center (e.g., Mayer et al. 2010). If the shocked region satisfies our post-shock criterion for the  $\text{H}_2$  collisional dissociation, the SMS formation is expected also in this case. In merging galaxies, however, star formation and also metal enrichment are expected to have already proceeded significantly. Therefore, in the case of the inflows by galaxy merger, SMS formation is probably prohibited by the metal-cooling effect. The cold accretion shocks in the first galaxy formation would provide more easily the suitable conditions for SMS formation. Recently, assuming seed BHs with  $\sim 10^5 M_\odot$ , Di Matteo et al. (2011) and Khandai et al. (2011) discussed their growth by the cold accretion flows in the process of the first galaxy formation. Their results demonstrate that the cold flows are less susceptible to feedbacks from the growing BHs and high accretion rate is maintained until mass of the galaxy reaches  $\gtrsim 10^{12} M_\odot$ , where the cold mode of accretion turns the usual hot virialization mode. As a result, the BH is able to grow to  $\gtrsim 10^9 M_\odot$  by  $z \sim 6$ . Our scenario for the SMS formation provides a mechanism for seeding BHs of  $\sim 10^5 M_\odot$  in forming galaxies, which has been assumed in studies of Di Matteo et al. (2011) and Khandai et al. (2011), while their results complementary demonstrated those seed BHs can in fact grow to SMBHs.

Finally, we remark remaining issues to be explored. In our scenario, the physical condition in the post-shock gas (especially, its density) is crucial for the SMS formation. We have considered a range of density ( $10^2 - 10^7 \text{ cm}^{-3}$ ) and temperature ( $3000 - 10^5 \text{ K}$ ) as the post-shock conditions. Currently, we only know the typical values of those parameters (Greif et al. 2008; Wise et al. 2008), but are still lacking knowledge of the relationship between the post-shock conditions and formation conditions (i.e., mass, virialization epoch, etc.) of first galaxies. In addition, our assumption that the enough mass supply for Jeans instability is available through the streaming flow is need further investigation. Safranek-Shrader et al. (2010) evaluated the amount of accreted gas to be  $\sim 10^5 M_\odot$ , which is inhomogeneously organized by turbulence (e.g., Wise & Abel 2007; Greif et al. 2008). Therefore, the outcome of the shocked material in most of halos could be numerous small sub-regions, rather than a massive layer envisaged in this paper. On the other hand, even if the turbulent motion dominates, a gravitational unstable cloud with  $\sim 10^5 M_\odot$  could form in the center and collapse subsequently (Wise et al. 2008). As a future project, we need to study in what halos the SMS forming conditions are satisfied by way of realistic cosmological simulations, including e.g., molecular cooling and the radiative and chemical feedbacks, for evaluating more quantitatively the feasibility of SMS formation in the first galaxies.

In this paper, we have supposed that, for the SMS formation, massive clouds must collapse isothermally without fragmentation. In fact, three-dimensional hydrodynamical simulations by Bromm & Loeb (2003) confirmed in some cases that the cloud collapsing isothermally by the atomic

cooling does not experience fragmentation at least in the range  $\lesssim 10^9 \text{ cm}^{-3}$  and, consequently, a supermassive clump forms at the center. Even with some angular momentum, fragmentation resulted at most in a binary system in their calculation. However, depending on such initial conditions as degrees of rotation or turbulence, the clouds would fragment into less massive clumps during the isothermal collapse. As a future study, it is awaited to clarify the conditions under which the clouds elude fragmentation by way of three-dimensional hydrodynamical calculation.

## ACKNOWLEDGMENTS

We would like to thank Takashi Nakamura for his continuous encouragement, and Takashi Hosokawa and Sanemichi Takahashi for the fruitful discussion. We also thank an anonymous referee for a careful reading of the manuscript and for constructive criticism that improved this paper. This work is in part supported by the Grants-in-Aid by the Ministry of Education, Culture, and Science of Japan (23-838 KI; 2168407 and 21244021 KO).

## REFERENCES

- Alvarez, M. A., Wise, J. H., & Abel, T. 2009, *ApJL*, 701, L133
- Bianchi, S., & Schneider, R. 2007, *MNRAS*, 378, 973
- Birnboim, Y., & Dekel, A. 2003, *MNRAS*, 345, 349
- Bromm, V., & Loeb, A. 2003, *ApJ*, 596, 34
- Bromm, V., & Yoshida, N. 2011, *ARA&A*, 49, 373
- Dekel, A., & Birnboim, Y. 2006, *MNRAS*, 368, 2
- Dekel, A., Birnboim, Y., Engel, G., et al. 2009, *Nature*, 457, 451
- Dijkstra, M., Haiman, Z., Mesinger, A., & Wyithe, J. S. B. 2008, *MNRAS*, 391, 1961
- Di Matteo, T., Khandai, N., DeGraf, C., et al. 2012, *ApJL*, 745, L29
- Fan, X. 2006, *New Astron Rev.*, 50, 665
- Greif, T. H., Johnson, J. L., Klessen, R. S., & Bromm, V. 2008, *MNRAS*, 387, 1021
- Greif, T. H., Glover, S. C. O., Bromm, V., & Klessen, R. S. 2010, *ApJ*, 716, 510
- Haiman, Z., & Loeb, A. 2001, *ApJ*, 552, 459
- Heger, A., & Woosley, S. E. 2002, *ApJ*, 567, 532
- Hollenbach, D., & McKee, C. F. 1989, *ApJ*, 342, 306
- Hosokawa, T., Omukai, K., Yoshida, N., & Yorke, H. W. 2011, *Science*, 334, 1250
- Inayoshi, K., & Omukai, K. 2011, *MNRAS*, 416, 2748
- Jeon, M., Pawlik, A. H., Greif, T. H., et al. 2011, *arXiv:1111.6305*
- Kang, H., & Shapiro, P. R. 1992, *ApJ*, 386, 432
- Kereš, D., Katz, N., Weinberg, D. H., & Davé, R. 2005, *MNRAS*, 363, 2
- Khandai, N., Feng, Y., DeGraf, C., Di Matteo, T., & Croft, R. A. C. 2011, *arXiv:1111.0692*
- Larson, R. B. 1969, *MNRAS*, 145, 271
- Larson, R. B. 1985, *MNRAS*, 214, 379
- Li, Y., et al. 2007, *ApJ*, 665, 187
- Mayer, L., Kazantzidis, S., Escala, A., & Callegari, S. 2010, *Nature*, 466, 1082



- Milosavljević, M., Couch, S. M., & Bromm, V. 2009, *ApJL*, 696, L146
- Mortlock, D. J., et al. 2011, *Nature*, 474, 616
- Nagakura, T., & Omukai, K. 2005, 364, 1378
- Nomoto, K., Tominaga, N., Umeda, H., Kobayashi, C., & Maeda, K. 2006, *Nuclear Physics A*, 777, 424
- Nozawa, T., Kozasa, T., & Habe, A. 2006, *ApJ*, 648, 435
- Omukai, K. 2001, *ApJ*, 546, 635
- Omukai, K., Schneider, R., & Haiman, Z. 2008, *ApJ*, 686, 801
- Penston, M. V. 1969, *MNRAS*, 144, 425
- Pollack, J. B., Hollenbach, D., Beckwith, S., Simonelli, D. P., Roush, T., & Fong, W. 1994, *ApJ*, 421, 615
- Regan, J. A., & Haehnelt, M. G. 2009a, *MNRAS*, 393, 858
- Regan, J. A., & Haehnelt, M. G. 2009b, *MNRAS*, 396, 343
- Safranek-Shrader, C., Bromm, V., & Milosavljević, M. 2010, *ApJ*, 723, 1568
- Shang, C., Bryan, G. L., & Haiman, Z. 2010, *MNRAS*, 402, 1249
- Shapiro, P. R., & Kang, H. 1987, *ApJ*, 318, 32
- Shibata, M., & Shapiro, S. L. 2002, *ApJL*, 572, L39
- Stacy, A., Greif, T. H., & Bromm, V. 2011, *arXiv:1109.3147*
- Uehara, H. & Inutsuka, S. 2000, *ApJ*, 531, L91
- Volonteri, M., Haardt, F., & Madau, P. 2003, *ApJ*, 582, 559
- Wise, J. H., & Abel, T. 2007, *ApJ*, 665, 899
- Wise, J. H., Turk, M. J., & Abel, T. 2008, *ApJ*, 682, 745
- Wise, J. H., Turk, M. J., Norman, M. L., & Abel, T. 2012, *ApJ*, 745, 50
- Willott, C. J., et al. 2007, *AJ*, 134, 2435
- Yamada, M., & Nishi, R. 1998, *ApJ*, 505, 148

This paper has been typeset from a  $\text{\LaTeX}$  file prepared by the author.